Journal of Interfaces, Thin films, and Low dimensional systems 6 (2) Winter and Spring (2023) 613-619

Thermal rectification in graphene/polyethylene junction: A molecular dynamics study

Scientific research paper

Leila Kiani[1], Javad Hasanzadeh[1*], Farrokh Yousefi[2], Peyman Azimi Anaraki[1]

[1]*Department of Physics, Takestan Branch, Islamic Azad University, Takestan, Iran*

[2]*Department of Physics, University of Zanjan, Zanjan, Iran*

ARTICLE INFO

Article history:
Received 10 June 2023
Revised 27 June 2023
Accepted 6 July 2023
Available online 22 November 2023

Keywords
Thermal rectification
Graphene
Polyethylene
Kapitza resistance
Molecular dynamics.

ABSTRACT

We use nonequilibrium molecular dynamics (NEMD) simulations to investigate thermal rectification in the graphene/polyethylene junction. An ultra-narrow zigzag graphene is connected to a polyethylene chain with a different number of monomers. We study the dependence of thermal rectification on the sample length (L) and mean temperature (T). Moreover, we calculate the Kapitza thermal resistance at the junction and show that it depends on the temperature gradient bias. The results show that thermal rectification weakly depends on the sample length. On the other hand, mean temperature suppresses thermal rectification and decreases with increasing temperature. Finally, to explore further, we calculate the phonon density of states (DOS) and study their scattering from the junction.

1 Introduction

Graphene [1,2] is a two-dimensional (2D) and nano-sized monolayer with a honeycomb form which has attracted many researchers in the past two decades due to uniquely high mechanical properties [3], excellent electronic or optical properties, and also thermal properties. Besides the remarkable properties of graphene, scientists also study the hybrid of graphene with other 2D or 3D materials to create new properties. An example of 3D, Razzaghi et al. used graphene as a nanofiller in polyethylene polymer (matrix) to enhance the thermal conductivity of the polymer [4]. The results indicate that the effective thermal conductivity of graphene-polyethylene nanocomposite (with a volume fraction of 1% graphene) increases to 0.74 W/mK, while that pure polyethylene has 0.36 W/mK.

Thermal rectification is an exotic thermal transport phenomenon which allows heat to transfer in one direction but blocks the other [5–9]. Thermal rectifiers can be made from a hybrid of two different materials [10–12], from mass graded [13–15], or asymmetry in the geometry of structure [16–20]. The hybrid of 2D materials can be an appropriate candidate for thermal rectifiers. In our previous work, we obtained thermal rectification of hybrid graphene/C3B [12]. In that study, the thermal rectification depends on the temperature difference between baths and increases by growing ΔT. The maximum thermal rectification that we got was equal to 48% for $\Delta T \geq 40$ K but zero rectification for $\Delta T < 40$ K.

In another work, Farzadian et al. studied the hybrid of graphene/C_3N to explore the thermal properties [10]. Thermal resistance and thermal rectification were important quantities that they investigated. In that system they obtained the thermal rectification factor about 50% around ΔT =100 K. Moreover, Rajabpour et al. showed that the hybrid of graphene and graphane

*Corresponding author.
Email address: javad.hasanzadeh@iau.ac.ir
DOI: 10.22051/jitl.2023.43819.1087

[21,22] is a promising thermal rectifier with 20% rectification for ΔT = 35 K for samples with a length of ≤ 100 nm [23]. Moreover, recently accurate potentials are developed with machine learning algorithms to study the same system, which can be useful for molecular dynamics simulations [24,25].

In the current work, we study the thermal properties of the hybrid of an ultra-narrow graphene with a polyethylene chain that includes a different number of monomers. We intend to calculate the thermal rectification in this class of hybrid systems. We also obtain thermal resistance and phonons density of states to explain the rectification mechanism.

2 Computational methods

The contribution of the phonon heat carriers in the semiconductors and nonconductors is greater than the electrons. Therefore, all the calculations in this study are based on the phonons. Consequently, we can ignore the electrons and use the NEMD simulations to obtain the thermal properties of the system. In this work, the simulations are implemented using the LAMMPS package as a classical molecular dynamics simulation code [26]. The simulated system is composed of ultra-narrow graphene attached to a polymer chain with 20 monomers, as shown in the schematic view in Fig. 1. The width of the graphene is 7.4 Å. The graphene/polyethylene length can be changed in different simulations.

The free boundary condition was applied to the three directions. To model the interaction between carbon and hydrogen atoms in the system, we chose the second-generation reactive empirical bond order (REBO) [27], which is a three-body potential.

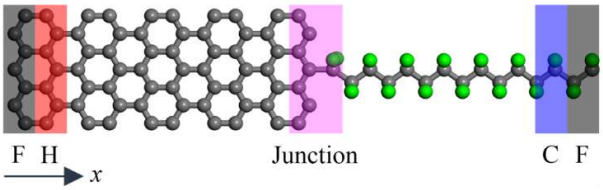

Figure 1. The schematic view of the simulated system. The F, H, and C represent fixed atoms, hot, and cold baths, respectively. hydrogen and carbon atoms are colored by grey and green, respectively.

The velocity Verlet algorithm was considered to integrate the equation of motion with a time step of 0.25 fs. At first, to relax and reach thermodynamic equilibrium, the whole of the system was coupled to the Langevin thermostat [28] at a specified temperature for 1 ns of simulation time. After that, as seen in Fig. 1, two narrow slabs, represented by F at two ends of the system, were selected as fixed atoms. Those atoms cannot move in all directions in the simulation time and operate as clamps. We placed the hot (H) and cold (C) baths near the fixed atoms.

At this step, we need a temperature gradient across the system. To build a temperature gradient, we applied a high temperature (T + ΔT/2) and a low temperature (T - ΔT/2) to the hot and cold baths, respectively. The temperature T is the mean temperature of the system, and ΔT is the temperature difference between the two heat sources (H and C). The Nose-Hoover thermostat [29,30] was applied to keep the temperature of the hot and cold baths constant. Also, the NVE ensemble was considered for atoms between the heat sources. In this condition, the temperature starts to fall along the system, and a temperature gradient is established. The system along the x direction was divided into few slabs with width of 1 nm to obtain the temperature profile. At those slabs, the temperature was calculated through the equipartition theorem and average for 2×10^6 of the last steps (equals 500 ps). The slope of the temperature profile is the effective temperature gradient. After building the temperature gradient, the heat current starts to reach a steady state in which the heat current magnitude is time-independent. Therefore, in this condition, the amount of heat extracted from the hot bath is equal to the added heat to the cold bath.

As we know, the applied thermostat continuously adds kinetic energy to the hot bath and removes it from the cold bath to keep those temperatures constant. The above energy gradually increases over time which is called accumulative energy. We obtain the accumulative energy and save it to calculate the baths' power or heat current. The heat current is used later for thermal rectification. To determine thermal rectification, we implement two simulations. The system was imposed to a positive temperature gradient and once again to a negative gradient. In both simulations, we calculate the heat current along the system. After that, thermal rectification was obtained via the equation below [6],

$$TR = \frac{J_{max} - J_{min}}{J_{min}} \times 100, \quad (1)$$

where J_{max} and J_{min} are the maximum and minimum heat currents between two directions of temperature gradients, respectively.

We finally calculate the phonon density of states (DOS) through Fourier transformation of the velocity autocorrelation. That is done by the equation below [31],

$$DOS(\omega) = \sum_s \frac{m_s}{k_B T} \int_0^\infty e^{-i\omega t} \langle \vec{v}(0).\vec{v}(t) \rangle_s dt, \quad (2)$$

where the summation is done on atom types s, and integration run over the simulation time. The m, v, ω are mass, velocity vector, and phonon angular frequency. The symbol $\langle ... \rangle$ demonstrates the velocity autocorrelation.

3 Results and discussion

All the NEMD simulations were carried out to explore the thermal rectification of the graphene/polyethylene junction. As demonstrated in Fig. 2, the temperature profiles for two biases of temperature gradient were plotted.

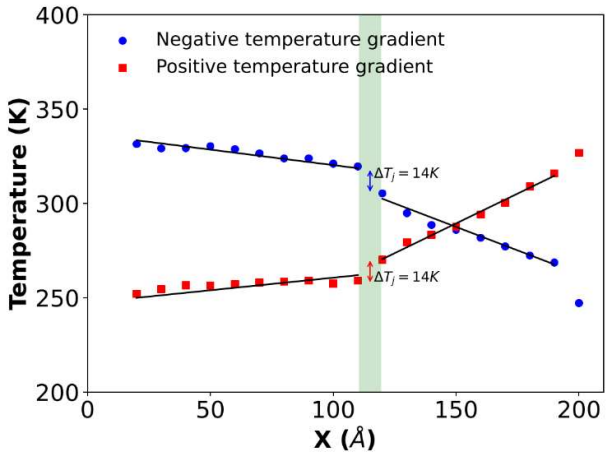

Figure 2. The temperature profile for negative (blue) and positive (red) temperature gradients. The interface is colored by light green. The length of the system is 20 nm. Also, T = 300 K and ΔT = 80 K.

We can see the temperature gap at the junction (colored by light green) in which temperature drops suddenly in a small region. The thermal resistance at the junction is related to the temperature gap at the interface, which will be explained later.

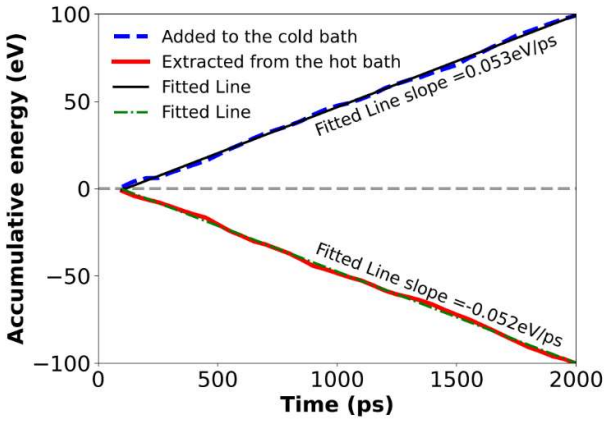

Figure 3. The accumulative energy extracted from the hot bath and added to the cold bath over the simulation time. The average of slope magnitude is the heat current. The length is 20 nm. Also, T = 300 K and ΔT = 80 K.

After that, we calculate the accumulative energy versus simulation time to obtain the heat current (energy/time). Two lines were fitted to the energy curves. The magnitude of the slope of the fitted lines should be approximately equal. That shows the system has reached a steady state. Therefore, the amount of energy that emerges from the hot bath equals with that entered into the cold bath. In this condition, we calculate thermal properties correctly.

Next, the thermal rectification was obtained through Eq. (1). As seen in Fig. 4. the thermal rectification weakly depends on the system length and fluctuates around 20% rectification. The length of the system varies up to 80 nm. The minimum and maximum rectification factors are equal to 18% and 23%. Therefore, we use it as a constant thermal. In the previous literature, it was illustrated that thermal rectification is independent of the length of the system [23].

Thermal rectification origins from the thermal resistance at the junction, the so-called Kapitza resistance [32]. The Kapitza resistance can be calculated as follows:

$$R_K = \frac{\Delta T_j}{J}, \quad (3)$$

where ΔT_j and J are the temperature gap at the junction and heat flux along the system, respectively.

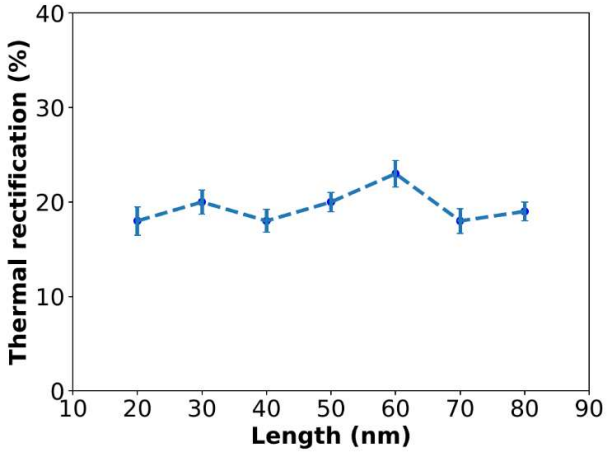

Figure 4. Thermal rectification at room temperature versus system length. T = 300 K and ΔT = 40 K.

Kapitza resistance depends on the temperature gradient. Therefore, thermal rectification occurs. To illustrate that, we compare Kapitza for a system with a length of 20 nm. When $\Delta T = 40K$, the temperature gap for two biases of the temperature gradient is equal ($\Delta T_j^{pos} \approx \Delta T_j^{neg} = 4.5\,K$), and also, the heat fluxes are $J_{pos} = 3.4e10\,W/m^2$ and $J_{neg} = 3.29e10\,W/m^2$. Therefore $R_K^{pos} = 1.32 \times 10^{-10} m^2K/W$ and $R_K^{neg} = 1.37 \times 10^{-10} m^2K/W$. Upon this calculation, Kapitza for the positive direction (graphene to polymer chain) is less than for the negative one. Therefore, the heat current prefers to flow in positive direction than negative direction. It leads to thermal rectification.

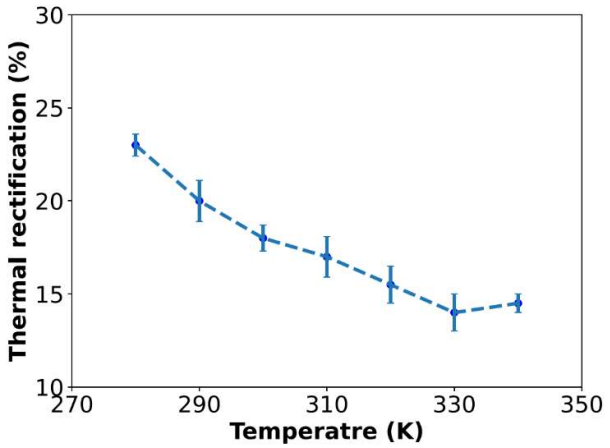

Figure 5. Thermal rectification vs mean temperature of the system.

Another quantity that can affect thermal rectification is the mean temperature of the sample. The mean temperature can be different in some environments. Therefore, it is important to explore the effect of temperature on thermal rectification. The temperature can affect the scattering phonons from the lattice and leads to a decrease in the heat current. Therefore, we expect the temperature to influence thermal rectification. As indicated in Fig. 5, the thermal rectification decreases with increasing temperature. The maximum and minimum thermal rectification are 23% and 14%, respectively. At low temperatures, the thermal rectification in the system can arise due to factors such as differences in phonon transport, asymmetric phonon scattering, or interface effects. These factors can lead to an asymmetry in how phonons propagate between materials or across interfaces, resulting in a preferential heat flow in one direction. This can give rise to a higher thermal conductance from the left side to the right side compared to the opposite direction, causing rectification. As the temperature increases, several mechanisms can contribute to decreasing thermal rectification. One possibility is that at higher temperatures, phonon-phonon interactions become more prevalent, and these interactions tend to equalize the heat flow between different materials or regions. As a result, the differences in phonon transport properties that caused rectification at lower temperatures become less pronounced.

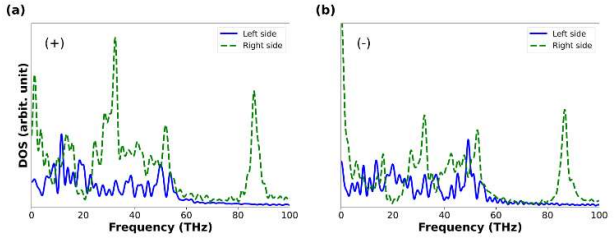

Figure 6. Phonon density of states of two groups of atoms near the junction in graphene (blue line) and polyethylene chain (green line) for heat flux in (+) and (-) directions.

To explore fundamentally and understand the observed thermal rectification, we obtained the phonon density of states (DOS) on both sides of the junction (Fig. 6). To do that, we selected two groups of atoms near the junction with a width of 20 Å. We obtained the velocity autocorrelation during the simulation time and then used Eq. (2) to calculate DOS. The mismatching between two DOS curves indicates that few modes of phonons exist on one side but not on the other. That means there is phonon scattering at the junction.

Now, we can calculate the overlapping factor between the two density of states on both sides of the junction using the following equation [6,33],

$$\Psi = \frac{\int_0^\infty D_1(\omega)D_2(\omega)d\omega}{\int_0^\infty D_1(\omega)d\omega \int_0^\infty D_2(\omega)d\omega}.$$

This quantity can be evaluated for positive and negative gradients. The overlapping factors are $\Psi_+ = 1.2635 \times 10^{-2}$ and $\Psi_- = 1.2098 \times 10^{-2}$, respectively.

4 Conclusions

We performed a series of NEMD simulations in the present investigation to calculate thermal rectification in the hybrid graphene/polyethylene chain. It was found that thermal rectification depends weakly on the system length. The magnitude of the thermal rectification is around 20%. To explain the underlying mechanism of thermal rectification, we calculated Kapitza resistance and phonon density of states on both sides of the junction. We showed that Kapitza resistance depends on the temperature gradient bias. Therefore, heat current prefers one direction (graphene to polyethylene chain) than the opposite direction. Moreover, the DOS was obtained to show some phonon modes scattering at the junction. The phonon scattering depends on the temperature gradient and leads to the Kapitza resistance.

Declaration of interest Statement

The authors declared that there is no conflict of interest.

References

[1] A. K. Geim, K. S. Novoselov, "The rise of graphene." Nature Materials, **6** (2007) 183–191. doi:10.1038/nmat1849.

[2] A. K. Geim, "Graphene: Status and prospects." Science, **324** (2009) 1530–1534. doi:10.1126/science.1158877.

[3] C. Lee, X. Wei, J. W. Kysar, J. Hone, "Measurement of the Elastic Properties and Intrinsic Strength of Monolayer Graphene." Science, **321** (2008) 385–388. doi:10.1126/science.1157996.

[4] L. Razzaghi, M. Khalkhali, A. Rajabpour, F. Khoeini, "Effect of graphene and carbon-nitride nanofillers on the thermal transport properties of polymer nanocomposites: A combined molecular dynamics and finite element study." Physical Review E, **103** (2021) 013310. doi:10.1103/PhysRevE.103.013310.

[5] R. Shrestha, Y. Luan, X. Luo, S. Shin, T. Zhang, P. Smith, W. Gong, M. Bockstaller, T. Luo, R. Chen, K. Hippalgaonkar, S. Shen, "Dual-mode solid-state thermal rectification." Nature Communications, **11** (2020) 4346. doi:10.1038/s41467-020-18212-2.

[6] F. Yousefi, F. Khoeini, A. Rajabpour, "Thermal conductivity and thermal rectification of nanoporous graphene: A molecular dynamics simulation." International Journal of Heat and Mass Transfer, **146** (2020) 118884. doi:10.1016/j.ijheatmasstransfer.2019.118884.

[7] X. Yang, D. Yu, B. Cao, A. C. To, "Ultrahigh thermal rectification in pillared graphene structure with carbon nanotube-graphene intramolecular junctions, ACS Applied Materials and Interfaces. **9** (2017) 29–35. doi:10.1021/acsami.6b12853.

[8] F. Yousefi, F. Khoeini, A. Rajabpour, "Thermal rectification and interfacial thermal resistance in hybrid pillared-graphene and graphene: a molecular dynamics and continuum approach." Nanotechnology. **31** (2020) 285707. doi:10.1088/1361-6528/ab8420.

[9] M. Sharifi, E. Heidaryan, "Thermal rectification in ultra-narrow hydrogen functionalized graphene: a non-equilibrium molecular dynamics study." Journal of Molecular Modelling, **28** (2022) 298. doi:10.1007/s00894-022-05306-5.

[10] O. Farzadian, A. Razeghiyadaki, C. Spitas, K. V Kostas, "Phonon thermal rectification in hybrid graphene-$\mathrm{C_{3}N}$: a molecular dynamics simulation." Nanotechnology. **31** (2020) 485401. doi:10.1088/1361-6528/abb04b.

[11] O. Farzadian, C. Spitas, K. V Kostas, "Graphene-carbon nitride interface-geometry effects on thermal rectification: a molecular

dynamics simulation." Nanotechnology. **32** (2021) 215403. doi:10.1088/1361-6528/abe786.

[12] L. Kiani, J. Hasanzadeh, F. Yousefi, P. A. Anaraki, "Phonon modes contribution in thermal rectification in graphene-C3B junction: A molecular dynamics study." Physica E Low-Dimensional Systems and Nanostructures. **131** (2021) 114724. doi:10.1016/j.physe.2021.114724.

[13] A. Saeedi, F. Yousefi Akizi, S. Khademsadr, M. Ebrahim Foulaadvand, "Thermal rectification of a single-wall carbon nanotube: A molecular dynamics study." Solid State Communications, **179** (2014) 54–58. doi:10.1016/j.ssc.2013.10.026.

[14] M. Romero-Bastida, M. Lindero-Hernández, "Thermal rectification in three-dimensional mass-graded anharmonic oscillator lattices." Physical Review E, **104** (2021) 044135. doi:10.1103/PhysRevE.104.044135.

[15] A. Tavakoli, J. Maire, B. Brisuda, T. Crozes, J.-F. Motte, L. Saminadayar, E. Collin, O. Bourgeois, Experimental evaluation of thermal rectification in a ballistic nanobeam with asymmetric mass gradient." Scientific Reports, **12** (2022) 7788. doi:10.1038/s41598-022-11878-2.

[16] F. Yousefi, M. Shavikloo, M. Mohammadi, "Non-equilibrium molecular dynamics study on radial thermal conductivity and thermal rectification of graphene." Molecular Simulation, **45** (2019) 646–651. doi:10.1080/08927022.2019.1578354.

[17] X. K. Chen, M. Pang, T. Chen, D. Du, K. Q. Chen, "Thermal Rectification in Asymmetric Graphene/Hexagonal Boron Nitride van der Waals Heterostructures. ACS Applied Materials and Interfaces, **12** (2020) 15517–15526. doi:10.1021/acsami.9b22498.

[18] A. Yousefzadi Nobakht, Y. Ashraf Gandomi, J. Wang, M. H. Bowman, D. C. Marable, B. E. Garrison, D. Kim, S. Shin, "Thermal rectification via asymmetric structural defects in graphene." Carbon, **132** (2018) 565–572. doi:10.1016/j.carbon.2018.02.087.

[19] X. Cartoixà, L. Colombo, R. Rurali, "Thermal Rectification by Design in Telescopic Si Nanowires." Nano Letters, **15** (2015) 8255–8259. doi:10.1021/acs.nanolett.5b03781.

[20] F. Rezaee, F. Yousefi, F. Khoeini, "Heat transfer in strained twin graphene: A non-equilibrium molecular dynamics simulation." Physica A Statistical Mechanics and its Applications, **564** (2021) 125542. doi:10.1016/j.physa.2020.125542.

[21] D. C. Elias, R. R. Nair, T. M. G. Mohiuddin, S. V. Morozov, P. Blake, M. P. Halsall, A. C. Ferrari, D. W. Boukhvalov, M. I. Katsnelson, A. K. Geim, K. S. Novoselov, "Control of Graphene's Properties by Reversible Hydrogenation: Evidence for Graphane." Science, **323** (2009) 610–613. doi:10.1126/science.1167130.

[22] A. K. Singh, B. I. Yakobson, "Electronics and Magnetism of Patterned Graphene Nanoroads." Nano Letters, **9** (2009) 1540–1543. doi:10.1021/nl803622c.

[23] A. Rajabpour, S. M. Vaez Allaei, F. Kowsary, "Interface thermal resistance and thermal rectification in hybrid graphene-graphane nanoribbons: A nonequilibrium molecular dynamics study." Applied Physics Letters, **99** (2011) 051917. doi:10.1063/1.3622480.

[24] B. Mortazavi, F. Shojaei, M. Shahrokhi, M. Azizi, T. Rabczuk, A. V. Shapeev, X. Zhuang, "Nanoporous C3N4, C3N5 and C3N6 nanosheets; novel strong semiconductors with low thermal conductivities and appealing optical/electronic properties." Carbon, **167** (2020) 40–50. doi:10.1016/j.carbon.2020.05.105.

[25] B. Mortazavi, E. V. Podryabinkin, S. Roche, T. Rabczuk, X. Zhuang, A. V. Shapeev, "Machine-learning interatomic potentials enable first-principles multiscale modeling of lattice thermal conductivity in graphene/borophene heterostructures." Materials Horizons, **7** (2020) 2359–2367. doi:10.1039/D0MH00787K.

[26] S. Plimpton, "Fast Parallel Algorithms for Short-Range Molecular Dynamics." Journal of

Computational Physics, **117** (1995) 1–19. doi:10.1006/jcph.1995.1039.

[27] D. W. Brenner, O. A. Shenderova, J. A. Harrison, S. J. Stuart, B. Ni, S. B. Sinnott, "A second-generation reactive empirical bond order (REBO) potential energy expression for hydrocarbons." Journal of Physics Condensed Matter, **14** (2002) 783–802. doi:10.1088/0953-8984/14/4/312.

[28] T. Schneider, E. Stoll, "Molecular-dynamics study of a three-dimensional one-component model for distortive phase transitions." Physical Review B, **17** (1978) 1302–1322. doi:10.1103/PhysRevB.17.1302.

[29] W. G. Hoover, "Canonical dynamics: Equilibrium phase-space distributions." Physical Review A, **31** (1985) 1695–1697. doi:10.1103/PhysRevA.31.1695.

[30] S. Nosé, "A unified formulation of the constant temperature molecular dynamics methods." Journal of Chemical Physics, **81** (1984) 511–519. doi:10.1063/1.447334.

[31] M. Khalkhali, F. Khoeini, "A. Rajabpour, Thermal transport in silicene nanotubes: Effects of length, grain boundary and strain." International Journal of Heat and Mass Transfer, **134** (2019) 503–510. doi:10.1016/j.ijheatmasstransfer.2019.01.074.

[32] H. Budd, J. Vannimenus, "Thermal Boundary Resistance." Physical Review Letters, **26** (1971) 1637–1640. doi:10.1103/PhysRevLett.26.1637.

[33] Y. Wang, A. Vallabhaneni, J. Hu, B. Qiu, Y. P. Chen, X. Ruan, "Phonon Lateral Confinement Enables Thermal Rectification in Asymmetric Single-Material Nanostructures." Nano Letters, **14** (2014) 592–596. doi:10.1021/nl403773f.